

### Reply to Anonymous Referee #3

We thank Anonymous Referee #3 for the valuable comments on our manuscript. Here we provide point-to-point responses to the Referees' comments. For clarity, the Referees' comments are marked in black, authors' responses are marked in **blue**, and changes in the manuscript are marked in **red**.

Hu et al. investigate the chemical composition, optical properties, and sources of aerosols (TSP and PM<sub>2.5</sub>) over the Bohai Sea (BS) and Yellow Sea (YS) during the summer of 2023. By combining bulk chemical analysis (ions, carbonaceous components), stable carbon isotopes ( $\delta^{13}\text{C}_{\text{TC}}$ ), and high-resolution mass spectrometry (Q-TOF MS) for molecular characterization, the authors provide an insight on how coastal terrestrial emissions impact the marginal sea atmospheres. It is an interesting study and the paper is well-written in general. I have some minor comments on the manuscript.

1. Title: I think that the authors have to revise the title of the manuscript to be more specific as 'coastal emissions' is too unclear and undefinable.

#### **Author reply:**

According to our research results, the term "Coastal emission" in the manuscript is intended to highlight terrestrial emissions from coastal provinces. Therefore, we ultimately revised the title to:

**Coastal terrestrial emissions modify the composition and optical properties of aerosols in marginal seas**

2. Line 23-24, Abstract: Suggest to revise the sentence. It is not clear how terrestrial emissions from coastal regions remain the major factor affecting marginal aerosols. Please be specific.

#### **Author reply:**

We have made revisions to the last sentence of the Abstract, emphasizing the terrestrial characteristics of aerosols and the sources of air masses (Page 1, Line 23–26).

Our results emphasize that during summer when the influence of marine air masses increases, the terrestrial characteristics of BS and YS aerosols remain evident, being related to air mass transport from coastal terrestrial regions.

3. Line 61: The term "weekly" seems inappropriate here. Did the authors mean "weakly"?

**Author reply:**

We thank the Referee for highlighting this error. It has been corrected to "weakly" in the revised manuscript. Page 2, Line 62–64:

In the BS and the northern YS heavily polluted by terrestrial sources, the formation pathway of atmospheric  $\text{NO}_3^-$  is dominated by anthropogenic hydrocarbon, which is significantly different from that in the southern YS, weakly influenced by terrestrial activities.

4. Lines 73-75: Sampling on the first deck of a research vessel is highly susceptible to the influence of the ship's own exhaust plumes. If any measures were taken to exclude self-contamination (e.g., wind sector control or BC filtering), please describe them in detail.

**Author reply:**

Placing the sampler on the first deck is currently a common practice for collecting field aerosols. The purpose of doing so is to keep the sampler as far away from the sea surface as possible, to avoid direct impact of splashing seawater on samples, and also to avoid the influence of ship exhaust at the stern. As for the wind sector control or BC filtering mentioned by the Referee, some studies have indeed adopted this method (Huang et al., 2022; Kim et al., 2015). However, this requires the sampler to be equipped with a wind direction monitoring device to prevent it from collecting airflow from the stern of the ship, or online aerosol mass spectrometer on board that can identify the sampling periods with high BC content. Here, we have taken another different preventive measure, namely the current common practice: instruments only collect samples during sailing (Song et al., 2018a; Zhao et al., 2024). Because only during the sailing of the

ship can it be ensured that the airflow comes as much as possible from the bow of the ship rather than the stern.

Details on avoiding the impact of ship emissions have been updated in the revised manuscript, Page 3, Line 78–79:

In order to avoid the impact of ship exhaust emissions and ensure that the collected airflow comes from the bow of the ship, the sampler only starts sampling when the ship is sailing.

5. Lines 126-127: In Equations (5) and (6), 72 hours is used as the time scale for weight decay. What is the basis for selecting 72 hours? Should different weighting factors be applied for substances with different atmospheric lifetimes?

**Author reply:**

The atmospheric lifetime of aerosols is the key factor determining whether they can affect the receptor sites. The selection of 72 hours as the transport time for air masses is mainly based on two basic reasons:

Firstly, previous studies showed that the atmospheric lifetime of aerosol chemical composition mainly varies on time scales of hours to a few days (Gao et al., 2022a). For example, early research suggested that the atmospheric lifetime of aerosols ranged from 4 to 60 days (Giorgi and Chameides, 1986), with aerosols confined in source regions having short atmospheric lifetimes and aerosols undergoing long-range transport having a longer atmospheric lifetime (Balkanski et al., 1993). Although there are differences in the evaluation results of different models for the atmospheric lifetime of organic and inorganic aerosols, there is relatively little difference in the time scale of atmospheric lifetime for the same type of aerosol/composition. The AeroCom Phase III model shows the global average lifetime of some inorganic components: nitrate at 2–7.8 days (mean of 5 days), ammonium at 1.9–9.8 days (mean of 4.3 days), sulfate at 0.86–7.6 days (mean of 4.5 days) (Bian et al., 2017; Park et al., 2004). For organic aerosols, the global average lifetime estimated based on the AeroCom Phase II model is 3.8–9.6 days (mean of 5.7 days) (Tsagaridis et al., 2014), while GEOS Chem simulated organic aerosol lifetime of about 4.9 and 5.8 days using two different

schemes (Pai et al., 2020). The more complex MAM7 reported lifetimes of 3.8 days for sulfate, 3.4 days for ammonium at, 5 days for primary organic matter (POM), 4.1 days for secondary organic aerosols, and 4.4 days for black carbon (Liu et al., 2012). Hence, using 72 hours (3 days) as the simulation time for air masses is generally appropriate. This time covers the atmospheric lifetimes of the above aerosol components or within their atmospheric lifetime.

Secondly, when conducting air mass trajectory analysis in marginal seas, current field studies usually set the simulation duration to 48 or 72 hours, though some studies even use longer simulation times (5 days or 10 days) (Mo et al., 2022; Budhavant et al., 2020; Li et al., 2023; Xu et al., 2025). Besides, previous studies using Eq. (7) and Eq. (8) in the main manuscript to calculate retention ratios and air masses also set the simulation duration to 72 hours (Zhou et al., 2023; Liu et al., 2022). Therefore, 72 hours was chosen for consistency with previous studies.

Finally, for the Referee's comment of applying different weighting factors, the original formula mainly aims to express that due to the diffusion and deposition of substances during transport, the longer the transport time, the weaker the impact on the recipient site. The calculation results are presented in the form of air mass retention ratio. If different time weighting factors are used for different substances, it will increase computational complexity. Besides, the atmospheric lifetimes of different substances are different. Calculating the air mass retention ratio of each substance separately may introduce significant uncertainties. Therefore, we uniformly used 72 hours as the time weighting factor to maintain consistency with literature data.

This has been updated in the revised manuscript, Page 6, Line 155–158:

Given that the average atmospheric lifetime of organic and inorganic substances in aerosols reported in literature is mainly around 3–6 days (Pai et al., 2020; Liu et al., 2012), and referring to the commonly used air mass simulation time (Cohen et al., 2015), we chose to simulate the trajectory of the air mass within 72 hours.

6. Lines 145-146: PMF models typically require a large sample size to ensure the stability of factorization. The manuscript notes that sampling occurred from July 15-23

and August 11-13, with TSP sampling durations of 12 h and PM5 of 24 h. This implies a relatively small total number of samples (roughly estimated at fewer than 30-40 valid samples). Resolving 4-5 factors with such a small sample size can lead to highly uncertain in the results. I suggest the author to include the results of residual analysis and other error analyses in the text.

**Author reply:**

Based on the Referee's comment, we have provided the error evaluation results and residual analysis of PMF in the Supplement. Table R1 shows the two error evaluation methods: Displacement (DISP) and Bootstrap (BS). The fact that no factors swaps are observed in DISP result indicates no significant rotational ambiguity and a relatively robust solution. BS results show that although not all of the base factors were mapped to the boot factors, matching rates of all factors are close to 100%, with only one factor having a low matching rate that still exceeds 80%. This indicates that the five-factor solution is relatively stable. The unmapped factors may be due to the combination of the high variability in the data and PMF not fitting all of the data.

We also verified the error evaluation results of the four-factor and six-factor solutions. The matching rate of each of these solutions (Table R2 and Table R3) is lower than that of the five-factor solution, and their Q(True)/Q(Robust) ratios are higher than that of the five-factor solution (Figure R1). Low Q(True)/Q(Robust) ratio is usually indicative of the reasonableness of the model results (Song et al., 2018b). Low Q(True)/Q(Robust) ratio and high matching rate indicate that five-factor solutions are more suitable than four-factors solutions. In addition, the fitting coefficients of each species in the five-factor solution are high enough (Table R4). The scaled residuals of all species in the five-factor solution are mainly within + 3 and - 3 (Figure R2), indicating that each species fits well in the model. Hence, we finally report the results of the five-factor solution.

Table R1. Results of two error estimation methods (Displacement: DISP, Bootstrap: BS) for a five-factor solution.

DISP Diagnostics	
Error Code:	0

Largest Decrease in Q:	-0.047					
%dQ:	-0.0071					
Swaps by Factor:	0	0	0	0	0	
BS Mapping						
	Base Factor 1	Base Factor 2	Base Factor 3	Base Factor 4	Base Factor 5	Unmapped
Boot Factor 1	96	0	2	1	1	0
Boot Factor 2	0	98	0	0	0	2
Boot Factor 3	1	0	99	0	0	0
Boot Factor 4	1	3	3	89	3	1
Boot Factor 5	0	0	0	0	100	0

Table R2. Results of two error estimation methods (Displacement: DISP, Bootstrap: BS) for a four-factor solution.

DISP Diagnostics						
Error Code:	0					
Largest Decrease in Q:	-0.056					
%dQ:	-0.0044					
Swaps by Factor:	0 0 0 0					
BS Mapping						
	Base Factor 1	Base Factor 2	Base Factor 3	Base Factor 4	Base Factor 5	Unmapped
Boot Factor 1	95	0	0	4	1	
Boot Factor 2	2	90	2	2	4	
Boot Factor 3	4	3	89	3	1	
Boot Factor 4	4	1	0	94	1	

Table R3. Results of two error estimation methods (Displacement: DISP, Bootstrap: BS) for a six-factor solution.

DISP Diagnostics							
Error Code:	0						
Largest Decrease in Q:	-0.011						
%dQ:	-0.030						
Swaps by Factor:	0 0 0 0 0 0						
BS Mapping							
	Base Factor 1	Base Factor 2	Base Factor 3	Base Factor 4	Base Factor 5	Base Factor 6	Unmapped
Boot Factor 1	97	0	2	1	0	0	0
Boot Factor 2	4	71	5	5	3	9	3
Boot Factor 3	5	2	84	3	2	4	0

Boot Factor 4	4	9	2	78	5	2	0
Boot Factor 5	0	0	0	0	100	0	0
Boot Factor 6	0	1	0	0	0	99	0

Table R4. Fitting results between observed concentration and predicted concentration of each species in the four to six-factor solutions.

Species	Four-factor solution	Five-factor solution	Six-factor solution
Particle	0.70	0.70	0.70
OC	0.86	0.94	0.97
EC	0.55	0.72	0.76
WSOC	0.96	0.97	0.98
HULIS	0.93	0.93	0.97
SOC	0.75	0.98	0.97
Na <sup>+</sup>	0.97	0.98	0.99
NH <sub>4</sub> <sup>+</sup>	0.98	0.98	0.98
K <sup>+</sup>	0.83	0.82	0.95
Mg <sup>2+</sup>	0.97	0.98	0.99
Ca <sup>2+</sup>	0.97	0.99	1.00
Cl <sup>-</sup>	0.95	0.97	0.98
NO <sub>3</sub> <sup>-</sup>	0.92	0.93	0.89
SO <sub>4</sub> <sup>2-</sup>	0.82	0.91	0.99
nss-K <sup>+</sup>	0.80	0.79	0.93
nss-Ca <sup>2+</sup>	0.96	0.99	1.00
nss-SO <sub>4</sub> <sup>2-</sup>	0.82	0.91	0.98

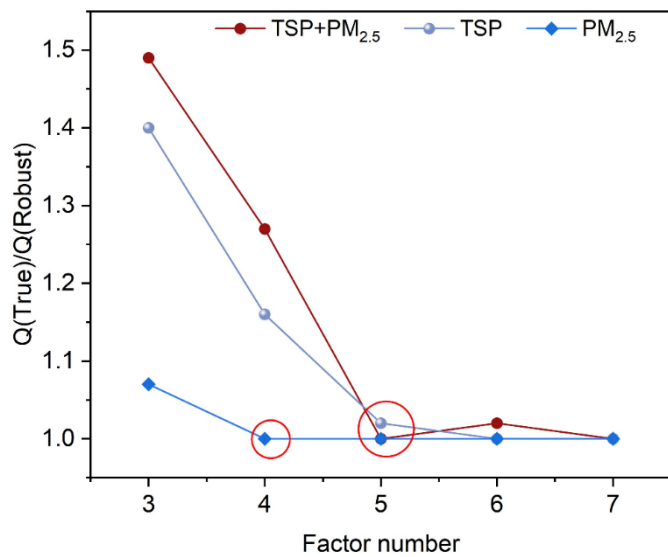


Figure R1. Variation of  $Q(\text{True})/Q(\text{Robust})$  with the increase of factor number. The red circles represent the optimal factor number.

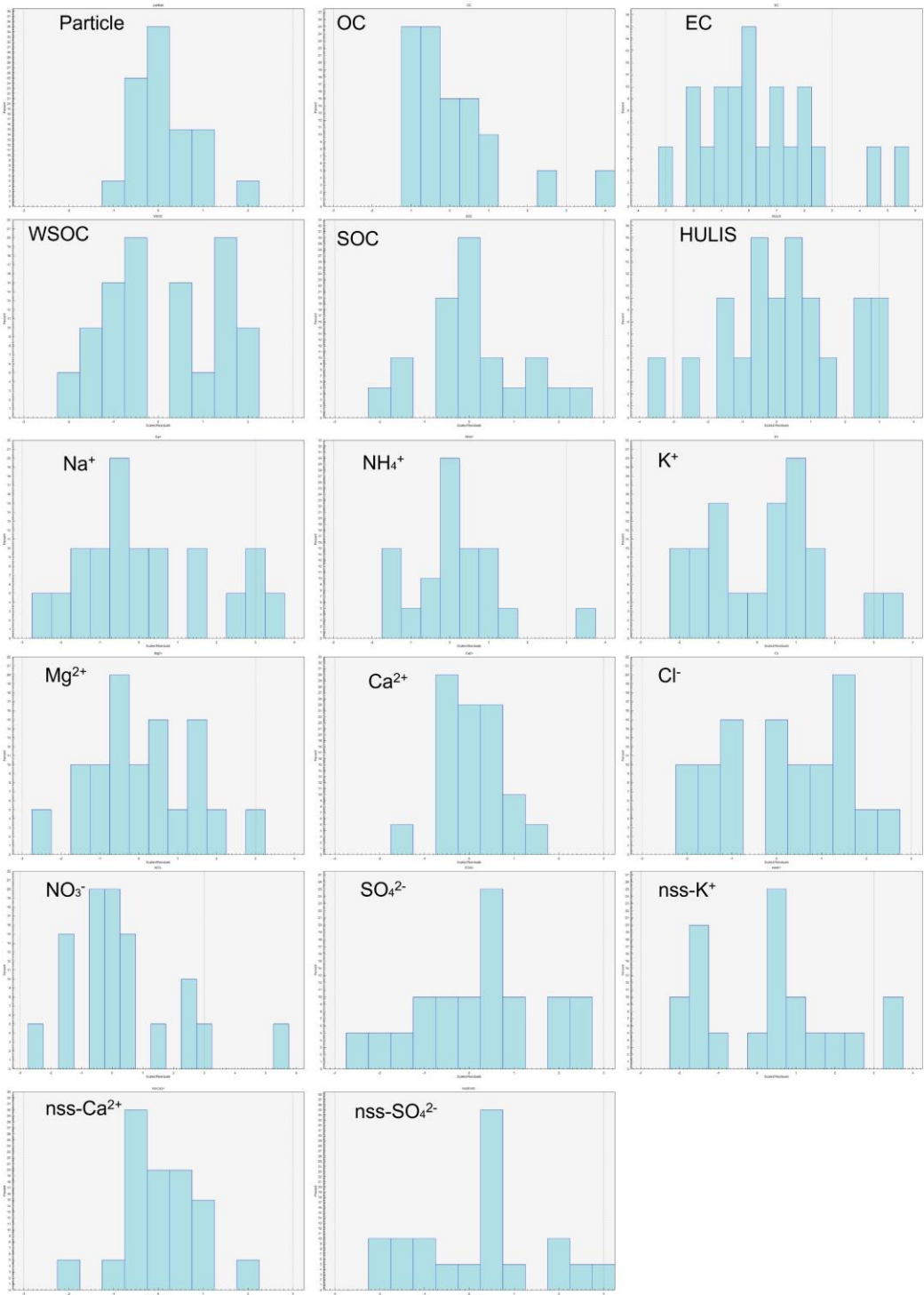


Figure R2. Residual distribution of each species in the five-factor solution.

To demonstrate the reliability of the PMF results, we have added an evaluation description of the model results (see Text S3), as well as corresponding residual and

error estimation result (Figure S18, Table S10 and Table S11) in the Supplement. Supplement, Page 6, Line 97–111:

As shown in Figure S17, the Q(True)/Q(Robust) ratio significantly decreases with the number of factors increasing to five, but it weakly decreases when the number of factors exceeds five. Besides, both error evaluation methods reveal that the five-factor solution is stable. No factors swaps were observed in the DISP result, which indicates no significant rotational ambiguity and that the solution is relatively robust (Table S10). BS results show that although not all of the base factors were mapped to the boot factors, matching rates of four factors are close to 100%, with only one factor having a low matching rate that still exceeds 80% (Table S10). This indicates that the five-factor solution is relatively stable. The unmapped factors may be due to the combination of the high variability in the data and PMF not fitting all of the data. In addition, the fitting coefficients ( $r^2$ ) of most species in the five-factor solution are higher than 0.9 (Table S11). The scaled residuals of all species are mainly within  $+ 3$  and  $- 3$  (Figure S18), indicating that each species fits well in the model. Hence, we finally report the results of five-factor solution.

7. Section 3.5: This manuscript will benefit more by further extending the discussion in this section. The current discussion is too simple and not detail enough. For example, what kind of combustion source and atmospheric secondary transformation in the atmosphere is plausible for influencing the marginal seas. Or further showing how important are these sources in this region. Are there any previous study supports the current PMF results and so on?

**Author reply:**

In this Section, we mainly analyzed in detail how to determine the source of aerosols based on the factor profile of PMF. Coming to the Referee's comment, we have identified that the combustion source may be from biomass, which is consistent with the analysis results based on  $\delta^{13}\text{C}_{\text{TC}}$ . As for the atmospheric secondary transformation, although we can determine which secondary species account for a larger proportion based on the factor profile, assessing the pathways through which these secondary

species are generated is beyond the scope of this study. Nevertheless, we briefly explored the possible formation pathways of secondary species reported in the literature. This has been updated in the revised manuscript, Page 14, Line 368–380:

The species with a high proportion in the profile of factor 1 is  $\text{Ca}^{2+}$  or  $\text{nss-Ca}^{2+}$ , which is commonly believed to originate from the crust or soil (Stanimirova et al., 2023). Therefore, this factor is identified as a dust source. The characteristic ion components in factor 2 are  $\text{Na}^+$ ,  $\text{Mg}^{2+}$  and  $\text{Cl}^-$ , with  $\text{Na}^+$  and  $\text{Cl}^-$  exhibiting the highest proportion (Zong et al., 2016). Therefore, this factor may be associated with sea salt and is identified as a marine primary source. Factor 3 has a high proportion of secondary inorganic ions ( $\text{NH}_4^+$  and  $\text{NO}_3^-$ ) derived from heterogeneous or homogeneous reaction of  $\text{NH}_3$  and  $\text{NO}_2$  (Pathak et al., 2009), and it is considered as a secondary inorganic source (Wei et al., 2024). Factor 4 has high proportions of EC, organic species,  $\text{nss-K}^+$  and  $\text{nss-SO}_4^{2-}$ . EC and  $\text{nss-K}^+$  jointly indicate that this factor may have connection with combustion source (biomass burning), while  $\text{nss-SO}_4^{2-}$  is associated with secondary transformation of  $\text{SO}_2$  (Dai et al., 2023; Xue et al., 2019). Hence, factor 4 is identified as mixture source (combustion source and  $\text{SO}_4^{2-}$ ). Factor 5, with a high proportion of SOC and low proportions of EC and inorganic species, is considered as a secondary organic source. The above proportions are consistent with results of previous studies conducted at BS and YS that have also shown that biomass combustion, secondary organic/inorganic aerosol sources, dust and sea salt are common sources of aerosol components (Zhao et al., 2023; Geng et al., 2020; Zhang et al., 2025).

8. References: Please edit on the formatting issues in the reference list.

**Author reply:**

We have checked and modified the format of the references.

9. Supporting Info, Figure S10: The figure resolution is low and the wording is too small. Please revise.

**Author reply:**

For clarity, the original figure has been split into the two separate figures below:

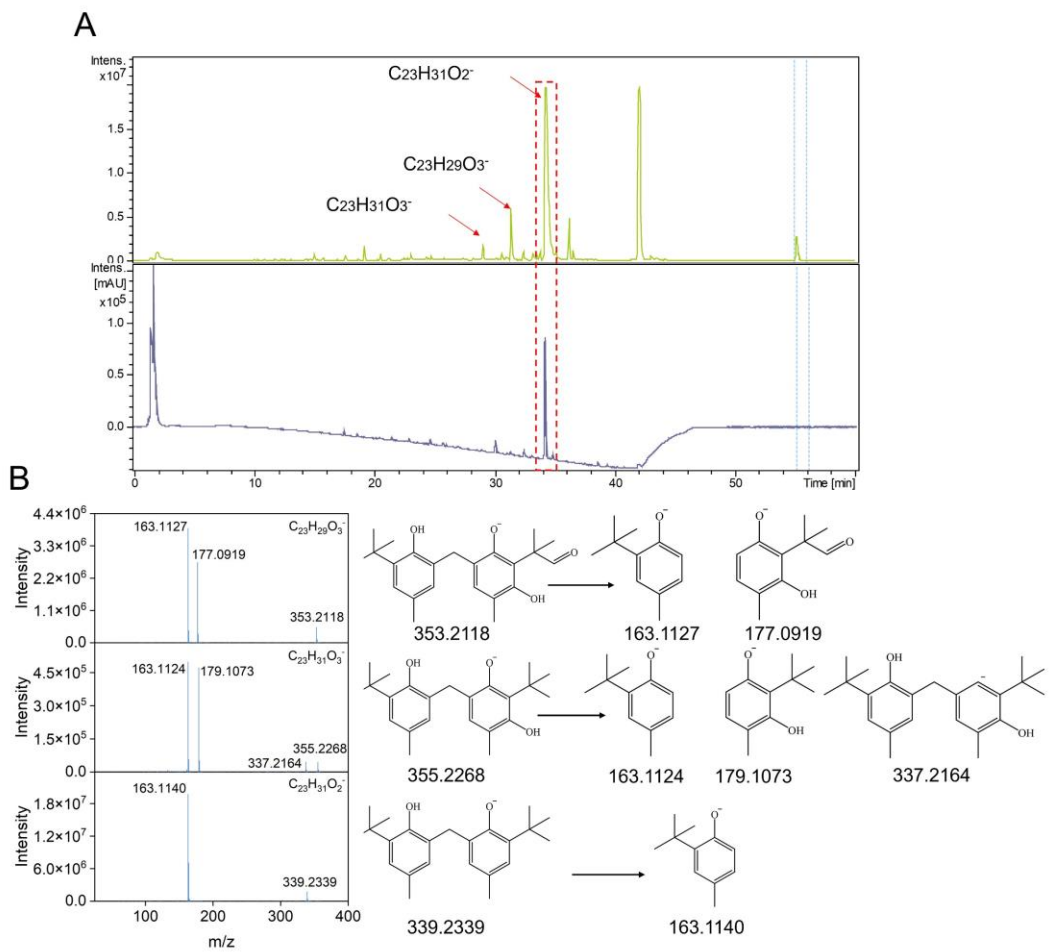


Figure S11. (A) Chromatographic peaks and light absorption chromatogram of  $\text{C}_{23}\text{H}_{31}\text{O}_2^-$  and its derivatives. The dotted lines represent the position of the mass spectrometry calibration solution. (B) Secondary mass spectra of  $\text{C}_{23}\text{H}_{31}\text{O}_2^-$  ( $m/z$ : 339.2339) and its derivatives and their possible structures.

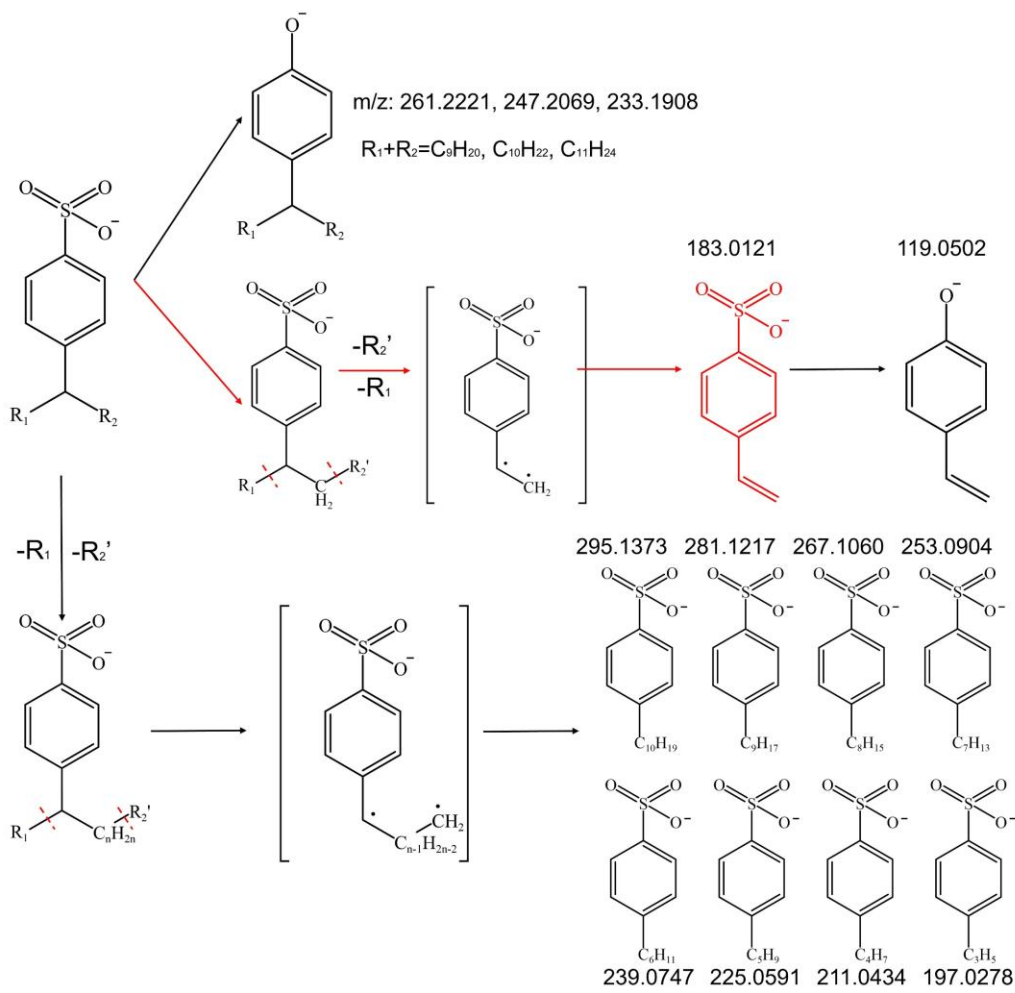
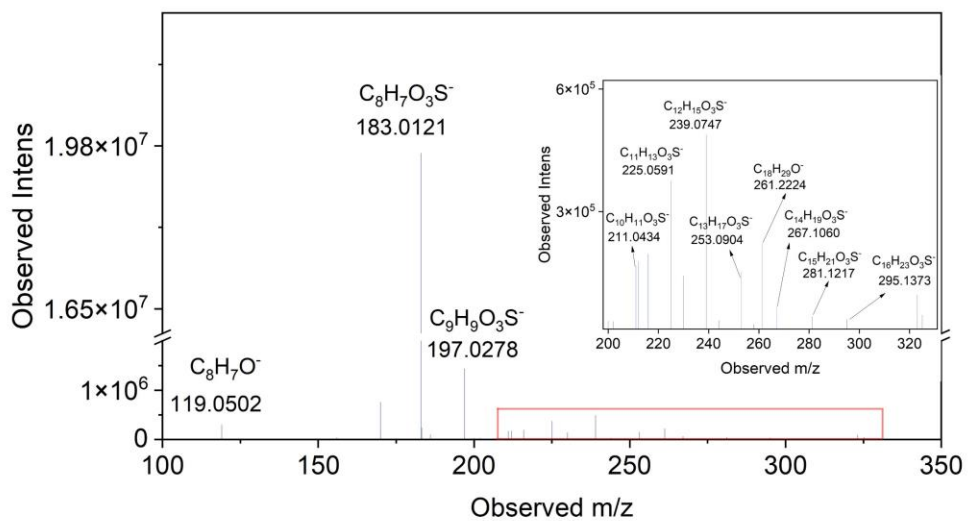


Figure S12. Secondary mass spectrometry of alkylbenzene sulfonic acid and its three fragmentation pathways. The red arrow and molecular formula represent the main fragmentation pathways and products. The red dashed line represents chemical bond breakage.

10. Supporting Info, Figure S12: What does the dotted line in the figure represent?

**Author reply:**

The dotted line in the Figure represents the position of the mass spectrometry calibration solution. Due to the fact that chromatographic peaks mainly occur in the first 50 minutes of gradient elution, we placed the calibration solution in the last few minutes of gradient elution during sample measurement, to ensure no interference with the analysis of sample chromatographic peaks. However, the mass spectrometry software (Bruker Compass DataAnalysis 4.2) we use cannot remove the two dotted lines. In order to avoid misunderstandings, we have provided explanations for these two dotted lines in the Figure caption. The modified Figure is as follows:

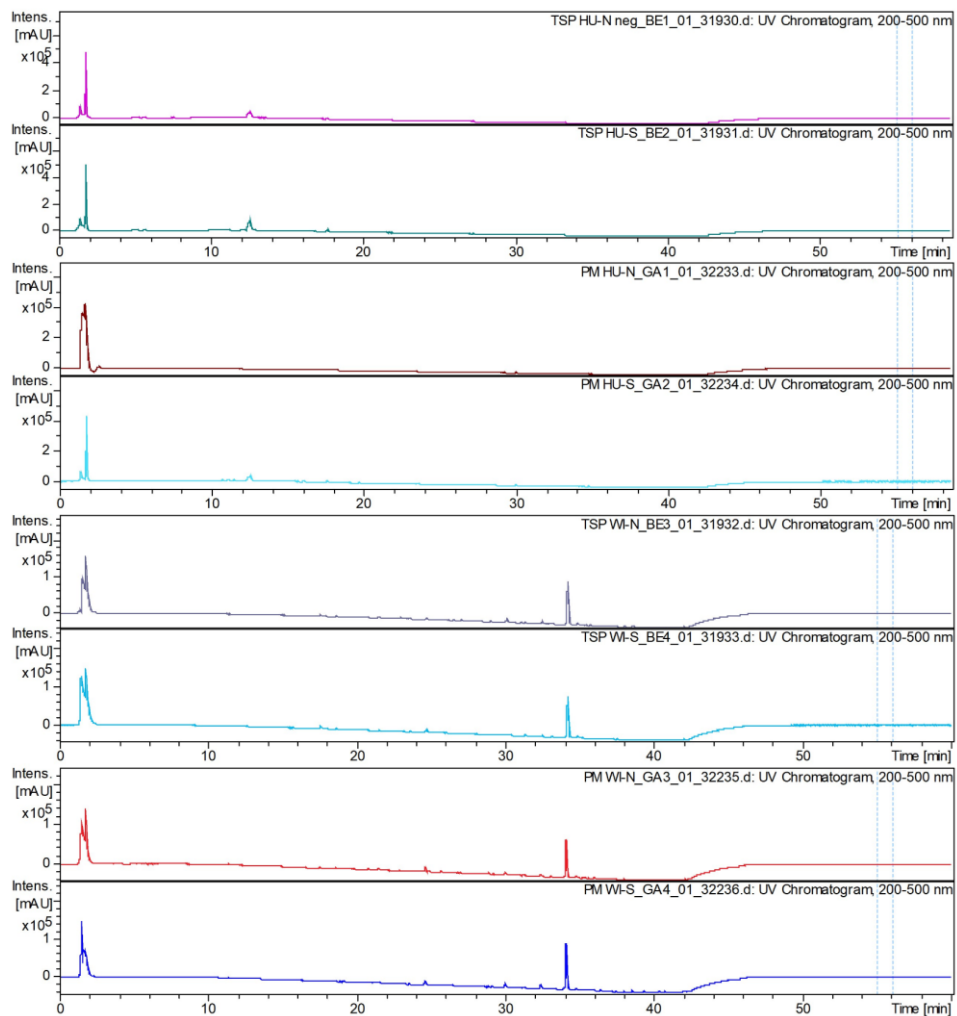


Figure S14. Absorption spectrum of HULIS and WISOC in the TSP and PM<sub>2.5</sub> samples. The dotted lines represent the position of the mass spectrometry calibration solution.

## References

Balkanski, Y. J., Jacob, D. J., Gardner, G. M., Graustein, W. C., and Turekian, K. K.: Transport and residence times of tropospheric aerosols inferred from a global three-dimensional simulation of  $^{210}\text{Pb}$ , *J. Geophys. Res.-Atmos.*, 98, 20573–20586, <https://doi.org/10.1029/93JD02456>, 1993.

Bian, H., Chin, M., Hauglustaine, D. A., Schulz, M., Myhre, G., Bauer, S. E., Lund, M. T., Karydis, V. A., Kucsera, T. L., Pan, X., Pozzer, A., Skeie, R. B., Steenrod, S. D., Sudo, K., Tsigaridis, K., Tsimpidi, A. P., and Tsyro, S. G.: Investigation of global particulate nitrate from the AeroCom phase III experiment, *Atmos. Chem. Phys.*, 17, 12911–12940, <https://doi.org/10.5194/acp-17-12911-2017>, 2017.

Budhavant, K., Andersson, A., Holmstrand, H., Bikkina, P., Bikkina, S., Satheesh, S. K., and Gustafsson, Ö.: Enhanced Light-Absorption of Black Carbon in Rainwater Compared With Aerosols Over the Northern Indian Ocean, *J. Geophys. Res.-Atmos.*, 125, e2019JD031246, <https://doi.org/10.1029/2019jd031246>, 2020.

Cohen, M. D., Stunder, B. J. B., Rolph, G. D., Draxler, R. R., Stein, A. F., and Ngan, F.: NOAA's HYSPLIT Atmospheric Transport and Dispersion Modeling System, *Bull. Amer. Meteorol. Soc.*, 96, 2059–2077, <https://doi.org/10.1175/bams-d-14-00110.1>, 2015.

Dai, Q., Chen, J., Wang, X., Dai, T., Tian, Y., Bi, X., Shi, G., Wu, J., Liu, B., Zhang, Y., Yan, B., Kinney, P. L., Feng, Y., and Hopke, P. K.: Trends of source apportioned  $\text{PM}_{2.5}$  in Tianjin over 2013–2019: Impacts of Clean Air Actions, *Environ. Pollut.*, 325, 121344, <https://doi.org/10.1016/j.envpol.2023.121344>, 2023.

Gao, C. Y., Heald, C. L., Katich, J. M., Luo, G., and Yu, F.: Remote Aerosol Simulated During the Atmospheric Tomography (ATom) Campaign and Implications for Aerosol Lifetime, *J. Geophys. Res.-Atmos.*, 127, e2022JD036524, <https://doi.org/10.1029/2022jd036524>, 2022a.

Geng, X., Mo, Y., Li, J., Zhong, G., Tang, J., Jiang, H., Ding, X., Malik, R. N., and Zhang, G.: Source apportionment of water-soluble brown carbon in aerosols over the northern South China Sea: Influence from land outflow, SOA formation and marine emission, *Atmos. Environ.*, 229, 117484, <https://doi.org/10.1016/j.atmosenv.2020.117484>, 2020.

Giorgi, F. and Chameides, W. L.: Rainout lifetimes of highly soluble aerosols and gases as inferred from simulations with a general circulation model, *J. Geophys. Res.-Atmos.*, 91, 14367–14376, <https://doi.org/10.1029/JD091iD13p14367>, 1986.

Huang, S., Wu, Z., Wang, Y., Poulain, L., Höpner, F., Merkel, M., Herrmann, H., and Wiedensohler, A.: Aerosol Hygroscopicity and its Link to Chemical Composition in a Remote Marine Environment Based on Three Transatlantic Measurements, *Environ. Sci. Technol.*, 56, 9613–9622, <https://doi.org/10.1021/acs.est.2c00785>, 2022.

Kim, G., Cho, H.-j., Seo, A., Kim, D., Gim, Y., Lee, B. Y., Yoon, Y. J., and Park, K.: Comparison of Hygroscopicity, Volatility, and Mixing State of Submicrometer Particles between Cruises over the Arctic Ocean and the Pacific Ocean, *Environ. Sci. Technol.*, 49, 12024–12035, <https://doi.org/10.1021/acs.est.5b01505>, 2015.

Li, H., Qin, X., Chen, J., Wang, G., Liu, C., Lu, D., Zheng, H., Song, X., Gao, Q., Xu, J., Zhu, Y., Liu, J., Wang, X., Deng, C., and Huang, K.: Continuous Measurement and Molecular Compositions of Atmospheric Water-Soluble Brown Carbon in the Nearshore Marine Boundary Layer of Northern China: Secondary Formation and Influencing Factors, *J. Geophys. Res.-Atmos.*, 128, e2023JD038565, <https://doi.org/10.1029/2023jd038565>, 2023.

Liu, C., Li, H., Zheng, H., Wang, G., Qin, X., Chen, J., Zhou, S., Lu, D., Liang, G., Song, X., Duan, Y., Liu, J., Huang, K., and Deng, C.: Ocean Emission Pathway and Secondary Formation Mechanism of Aminiums Over the Chinese Marginal Sea, *J. Geophys. Res.-Atmos.*, 127, e2022JD037805, <https://doi.org/10.1029/2022jd037805>, 2022.

Liu, X., Easter, R. C., Ghan, S. J., Zaveri, R., Rasch, P., Shi, X., Lamarque, J. F., Gettelman, A., Morrison, H., Vitt, F., Conley, A., Park, S., Neale, R., Hannay, C., Ekman, A. M. L., Hess, P., Mahowald, N., Collins, W., Iacono, M. J., Bretherton, C. S., Flanner, M. G., and Mitchell, D.: Toward a minimal representation of aerosols in climate models: description and evaluation in the Community Atmosphere Model CAM5, *Geosci. Model Dev.*, 5, 709–739, <https://doi.org/10.5194/gmd-5-709-2012>, 2012.

Mo, Y., Zhong, G., Li, J., Liu, X., Jiang, H., Tang, J., Jiang, B., Liao, Y., Cheng, Z., and Zhang, G.: The Sources, Molecular Compositions, and Light Absorption Properties of Water-Soluble Organic Carbon in Marine Aerosols From South China Sea to the Eastern Indian Ocean, *J. Geophys. Res.-Atmos.*, 127, e2021JD036168, <https://doi.org/10.1029/2021jd036168>, 2022.

Pai, S. J., Heald, C. L., Pierce, J. R., Farina, S. C., Marais, E. A., Jimenez, J. L., Campuzano-Jost, P., Nault, B. A., Middlebrook, A. M., Coe, H., Shilling, J. E., Bahreini, R., Dingle, J. H., and Vu, K.: An evaluation of global organic aerosol schemes using airborne observations, *Atmos. Chem. Phys.*, 20, 2637–2665, <https://doi.org/10.5194/acp-20-2637-2020>, 2020.

Park, R. J., Jacob, D. J., Field, B. D., Yantosca, R. M., and Chin, M.: Natural and transboundary pollution influences on sulfate-nitrate-ammonium aerosols in the United States: Implications for policy, *J. Geophys. Res.-Atmos.*, 109, D15204, <https://doi.org/10.1029/2003jd004473>, 2004.

Pathak, R. K., Wu, W. S., and Wang, T.: Summertime PM<sub>2.5</sub> ionic species in four major cities of China: nitrate formation in an ammonia-deficient atmosphere, *Atmos. Chem. Phys.*, 9, 1711–1722, <https://doi.org/10.5194/acp-9-1711-2009>, 2009.

Song, J., Zhao, Y., Zhang, Y., Fu, P., Zheng, L., Yuan, Q., Wang, S., Huang, X., Xu, W., Cao, Z., Gromov, S., and Lai, S.: Influence of biomass burning on atmospheric aerosols over the western South China Sea: Insights from ions, carbonaceous fractions and stable carbon isotope ratios, *Environ. Pollut.*, 242, 1800–1809, <https://doi.org/10.1016/j.envpol.2018.07.088>, 2018a.

Song, M., Tan, Q., Feng, M., Qu, Y., Liu, X., An, J., and Zhang, Y.: Source Apportionment and Secondary Transformation of Atmospheric Nonmethane Hydrocarbons in Chengdu, Southwest China, *J. Geophys. Res.-Atmos.*, 123, 9741–9763, <https://doi.org/10.1029/2018jd028479>, 2018b.

Stanimirova, I., Rich, D. Q., Russell, A. G., and Hopke, P. K.: A long-term, dispersion normalized PMF source apportionment of PM<sub>2.5</sub> in Atlanta from 2005 to 2019, *Atmos. Environ.*, 312, 120027, <https://doi.org/10.1016/j.atmosenv.2023.120027>, 2023.

Tsigaridis, K., Daskalakis, N., Kanakidou, M., Adams, P. J., Artaxo, P., Bahadur, R., Balkanski, Y., Bauer, S. E., Bellouin, N., Benedetti, A., Bergman, T., Berntsen, T. K., Beukes, J. P., Bian, H., Carslaw, K. S., Chin, M., Curci, G., Diehl, T., Easter, R. C., Ghan, S. J., Gong, S. L., Hodzic, A., Hoyle, C. R., Iversen, T., Jathar, S., Jimenez, J. L., Kaiser, J. W., Kirkevåg, A., Koch, D., Kokkola, H., Lee, Y. H., Lin, G., Liu, X., Luo, G., Ma, X., Mann, G. W., Mihalopoulos, N., Morcrette, J. J., Müller, J. F., Myhre, G., Myriocephalitakis, S., Ng, N. L., O'Donnell, D., Penner, J. E., Pozzoli, L., Pringle, K. J., Russell, L. M., Schulz, M., Sciare, J., Seland, Ø., Shindell, D. T., Sillman, S., Skeie, R. B., Spracklen, D., Stavrakou, T., Steenrod, S. D., Takemura, T., Tiitta,

P., Tilmes, S., Tost, H., van Noije, T., van Zyl, P. G., von Salzen, K., Yu, F., Wang, Z., Wang, Z., Zaveri, R. A., Zhang, H., Zhang, K., Zhang, Q., and Zhang, X.: The AeroCom evaluation and intercomparison of organic aerosol in global models, *Atmos. Chem. Phys.*, 14, 10845–10895, <https://doi.org/10.5194/acp-14-10845-2014>, 2014.

Wei, Y., Wang, S., Jiang, N., Zhang, D., and Zhang, R.: Study on main sources of aerosol pH and new methods for additional reduction of PM<sub>2.5</sub> during winter severe pollution: Based on the PMF-GAS model, *J. Clean Prod.*, 471, 143401, <https://doi.org/10.1016/j.jclepro.2024.143401>, 2024.

Xu, F., Hu, K., Lu, S. H., Guo, S., Wu, Y. C., Xie, Y., Zhang, H. H., and Hu, M.: Enhanced Marine VOC Emissions Driven by Terrestrial Nutrient Inputs and Their Impact on Urban Air Quality in Coastal Regions, *Environ. Sci. Technol.*, 59, 8140–8154, <https://doi.org/10.1021/acs.est.4c12655>, 2025.

Xue, J., Yu, X., Yuan, Z., Griffith, S. M., Lau, A. K. H., Seinfeld, J. H., and Yu, J. Z.: Efficient control of atmospheric sulfate production based on three formation regimes, *Nat. Geosci.*, 12, 977–982, <https://doi.org/10.1038/s41561-019-0485-5>, 2019.

Zhang, Y., Wang, Y., Li, S., Yi, Y., Guo, Y., Yu, C., Jiang, Y., Ni, Y., Hu, W., Zhu, J., Qi, J., Shi, J., Yao, X., and Gao, H.: Sources and Optical Properties of Marine Organic Aerosols Under the Influence of Marine Emissions, Asian Dust, and Anthropogenic Pollutants, *J. Geophys. Res.-Atmos.*, 130, e2025JD043472, <https://doi.org/10.1029/2025jd043472>, 2025.

Zhao, S., Qi, J., and Ding, X.: Characteristics, seasonal variations, and dry deposition fluxes of carbonaceous and water-soluble organic components in atmospheric aerosols over China's marginal seas, *Mar. Pollut. Bull.*, 191, 114940, <https://doi.org/10.1016/j.marpolbul.2023.114940>, 2023.

Zhao, Z. Y., Zhang, Y. L., Lin, Y. C., Song, W. H., Yu, H. R., Fan, M. Y., Hong, Y. H., Yang, X. Y., Li, H. Y., and Cao, F.: Continental Emissions Influence the Sources and Formation Mechanisms of Marine Nitrate Aerosols in Spring Over the Bohai Sea and Yellow Sea Inferred From Stable Isotopes, *J. Geophys. Res.-Atmos.*, 129, e2023JD040541, <https://doi.org/10.1029/2023jd040541>, 2024.

Zhou, S., Chen, Y., Wang, F., Bao, Y., Ding, X., and Xu, Z.: Assessing the Intensity of Marine Biogenic Influence on the Lower Atmosphere: An Insight into the Distribution of Marine Biogenic Aerosols over the Eastern China Seas, *Environ. Sci. Technol.*, 57, 12741–12751, <https://doi.org/10.1021/acs.est.3c04382>, 2023.

Zong, Z., Wang, X., Tian, C., Chen, Y., Qu, L., Ji, L., Zhi, G., Li, J., and Zhang, G.: Source apportionment of PM<sub>2.5</sub> at a regional background site in North China using PMF linked with radiocarbon analysis: insight into the contribution of biomass burning, *Atmos. Chem. Phys.*, 16, 11249–11265, <https://doi.org/10.5194/acp-16-11249-2016>, 2016.